Enzyme Inhibition

DOI: 10.1002/anie.201403540

para-Nitroblebbistatin, the Non-Cytotoxic and Photostable Myosin II Inhibitor**

*Miklós Képiró, Boglárka H. Várkuti, László Végner, Gergely Vörös, György Hegyi, Máté Varga, and András Málnási-Csizmadia**

Abstract: *Blebbistatin, the best characterized myosin II-inhibitor, is commonly used to study the biological roles of various myosin II isoforms. Despite its popularity, the use of blebbistatin is greatly hindered by its blue-light sensitivity, resulting in phototoxicity and photoconversion of the molecule. Additionally, blebbistatin has serious cytotoxic side effects even in the absence of irradiation, which may easily lead to the misinterpretation of experimental results since the cytotoxicity-derived phenotype could be attributed to the inhibition of the myosin II function. Here we report the synthesis as well as the in vitro and in vivo characterization of a photostable, C15 nitro derivative of blebbistatin with unaffected myosin II inhibitory properties. Importantly, para-nitroblebbistatin is neither phototoxic nor cytotoxic, as shown by cellular and animal tests; therefore it can serve as an unrestricted and complete replacement of blebbistatin both in vitro and in vivo.*

Blebbistatin is a cell-permeable, specific inhibitor of class II myosins, a group of actin-based ATP-driven motor proteins responsible for various biological processes including muscle contraction, cell migration, differentiation, and cytokinesis.[1] Since blebbistatin is the best characterized myosin II-specific inhibitor, it rapidly became the compound of choice to inhibit myosin II-dependent processes in different species and cell types, e.g. in cancer research and developmental biology, and in the field of cell motility.[2] A well-known limitation of blebbistatin treatment is the phototoxicity of the inhibitor upon blue-light illumination,[3] which causes structural changes in the molecule accompanied by the generation of reactive oxygen species responsible for the phototoxic effect.[3c]

The blue-light susceptibility of blebbistatin greatly hinders in vivo imaging, because excitation wavelengths below 500 nm seriously damage the blebbistatin-treated samples.[4] Additionally, incubation with blebbistatin exerts a significant cytotoxic effect even without irradiation,[3c] which causes serious problems in several in vivo systems. Further difficulties may arise from blebbistatin's own fluorescence, which interferes with fluorescent signals such as that from the green fluorescent protein (GFP) and with Förster resonance energy transfer (FRET) experiments.[5] For in vivo applications of blebbistatin, optimization of its chemical structure is essential. Introduction of a nitro group at the C7 position (Scheme 1) of the tricyclic core of blebbistatin (**7**) led to slightly decreased fluorescence and increased photostability.[6] However, the biological application of this blebbistatin derivative was hampered by its strongly decreased binding constant and specificity to myosin II. Recently, we reported a highly myosin II-specific, photoinducible, C15-substituted azido derivative of blebbistatin, called *para*-azidoblebbistatin,[7] which forms covalent cross-links with its target proteins upon UV and bluelight irradiation. We observed that *para*-azidoblebbistatin—unlike blebbistatin—is nonfluorescent

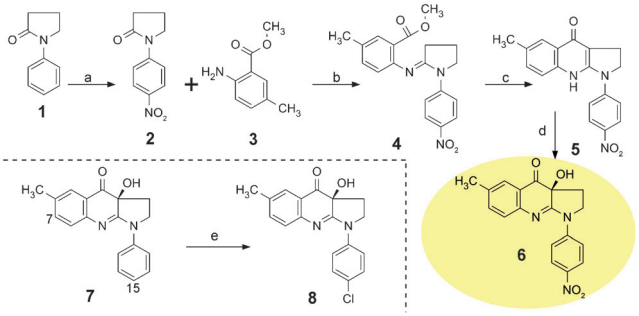

Scheme 1. Synthesis of *para*-nitroblebbistatin (**6**) and *para*-chloroblebbistatin (**8**). Reagents and conditions: a) H_2SO_4, HNO_3, 0 °C, 15 min; b) $POCl_3$, CH_2Cl_2, 50 °C, 18 h; c) LiHMDS, −78 °C to 0 °C, 3 h; d) oxaziridine, −10 °C, 16 h; e) $BF_3{\cdot}2H_2O$, CH_3OH, *N*-chlorosuccinimide, 100 °C microwave 30 min. The substituted positions applied in Ref. [6] (C7) and the present study (C15) are indicated in blebbistatin (**7**) (for detailed synthesis protocols see the Supporting Information).

[*] G. Hegyi, A. Málnási-Csizmadia
MTA-ELTE Molecular Biophysics Research Group (Hungary)
E-mail: malnalab@yahoo.com
Homepage: http://www.malnalab.hu
M. Képiró,[+] B. H. Várkuti,[+] L. Végner, G. Vörös, A. Málnási-Csizmadia
Department of Biochemistry, Eötvös Loránd University
Pázmány Péter sétány 1/c, 1117 Budapest (Hungary)
M. Varga
Department of Genetics, Eötvös Loránd University
Pázmány Péter sétány 1/c, 1117 Budapest (Hungary)
A. Málnási-Csizmadia
Drugmotif Ltd., Szt Erszebet krt 11, 2112 Veresegyhaz (Hungary)
[+] These authors contributed equally to this work.

[**] We are grateful to Mihaly Kovacs for his valuable comments. This work was funded by the European Research Council (European Community's Seventh Framework Programme (FP7/2007-2013)/ERC grant agreement no. 208319), ERC-PoC (grant agreement no. 620315), and Hungarian Research and Innovation Fund (KTIA_AIK_12-1-2013-0005). M.V. is a János Bolyai Fellow of the Hungarian Academy of Sciences. B.H.V. was supported by the European Union and the State of Hungary, cofinanced by the European Social Fund in the framework of TÁMOP 4.2.4. A/1-11-1-2012-0001 "National Excellence Program".

Supporting information for this article is available on the WWW under http://dx.doi.org/10.1002/anie.201403540.

 © 2014 Wiley-VCH Verlag GmbH & Co. KGaA, Weinheim

and non-cytotoxic. These findings and the electrochemical properties of the azido group initiated the idea that a C15 nitro- or chloro-substituted blebbistatin derivative (*para*-nitroblebbistatin or *para*-chloroblebbistatin) could be a non-photoreactive, and similarly non-cytotoxic and non-fluorescent myosin II-specific inhibitor. The replacement of blebbistatin by such a derivative in biological experiments would be advantageous. Below we demonstrate that by means of the C15 nitro substitution (Scheme 1) we managed to eliminate the fluorescence, photosensitivity, and photo- and cytotoxicity of blebbistatin without affecting its in vitro and in vivo inhibitory properties. We also present the structural model of *para*-nitroblebbistatin in complex with myosin II in which blebbistatin is extended by a nitro group at the C15 position in the atomic structural model of the blebbistatin–myosin complex (PDB: 1YV3).[8]

We synthesized *para*-nitroblebbistatin (**6**) by nitration of the pyrrolidinone building block of blebbistatin and subsequent application of Davis' oxaziridine protocol[6] (Scheme 1). *para*-Chloroblebbistatin (**8**) was synthesized by the direct chlorination of blebbistatin (**7**).

The strong fluorescence of blebbistatin is a serious limitation in fluorescent microscopy. In contrast, significantly reduced fluorescence characterizes *para*-nitroblebbistatin and *para*-chloroblebbistatin, as their emission intensity is less than 1% of that of blebbistatin (Figure 1A and Figure S1A).

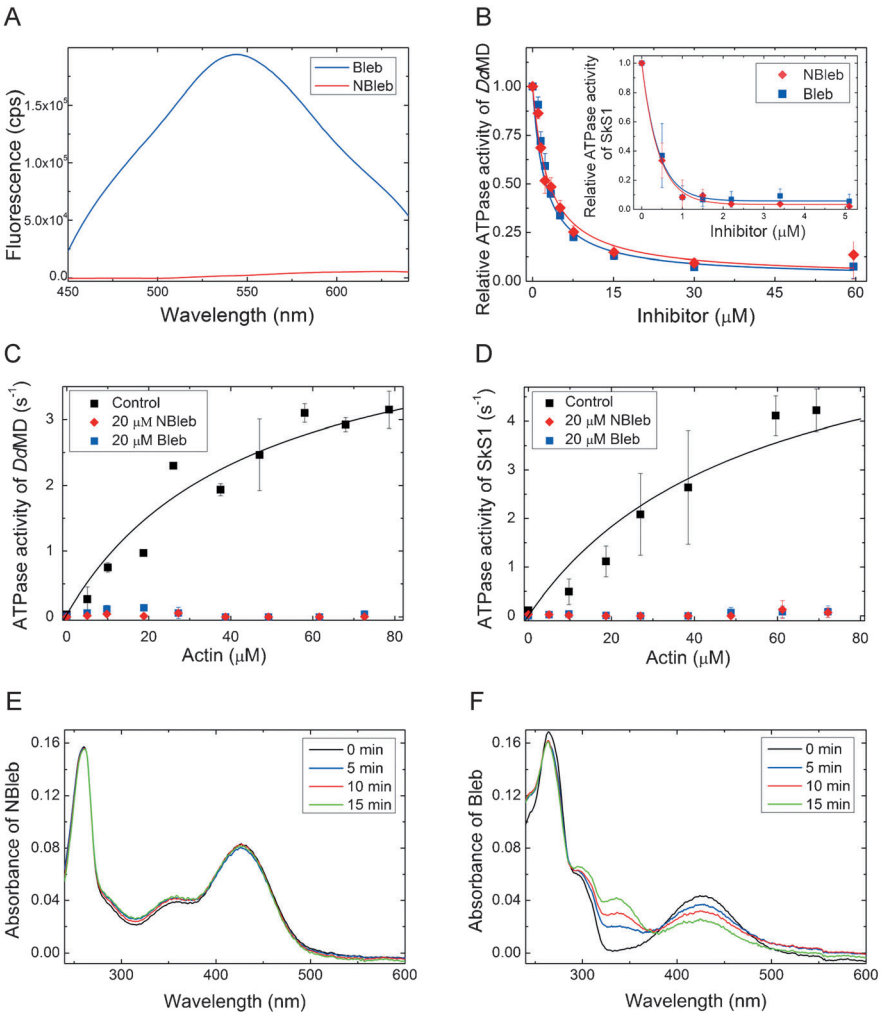

Figure 1. In vitro characterization of *para*-nitroblebbistatin (NBleb) and blebbistatin (Bleb). A) The fluorescence emission spectra of NBleb and Bleb were recorded using an excitation wavelength of 430 nm. B) The inhibition of the relative basal ATPase activities of *Dd*MD and SkS1 (inset) myosin II isoforms were recorded at increasing concentrations of NBleb and Bleb. The inhibition of actin-activated ATPase activities of C) *Dd*MD and D) SkS1 were measured at an inhibitor concentration of 20 μM in the presence of increasing concentrations of actin. Data represents the mean values ± standard deviation of three independent experiments. Photoconversion of E) NBleb and F) Bleb were followed by measuring their absorbance spectra after irradiation at 480 ± 10 nm at the indicated times.

The in vitro inhibitory effect of the derivatives was evaluated on the *Dictyostelium discoideum* myosin II motor domain (*Dd*MD) and the rabbit skeletal muscle myosin S1 (SkS1). The half maximal inhibitory concentration (IC_{50}) of the basal ATPase activity of *para*-nitroblebbistatin was the same as that of blebbistatin on *Dd*MD (2.33 ± 0.13 μM and 2.96 ± 0.45 μM, respectively) as well as on SkS1 (0.4 ± 0.05 μM and 0.41 ± 0.03 μM, respectively; Figure 1B). Both inhibitors completely suppressed actin activation of the myosin ATPase activity even at high concentrations of actin (80 μM) on both types of myosin isoforms (Figure 1C,D). Since the inhibitory properties of *para*-chloroblebbistatin and *para*-nitroblebbistatin are very similar, these results confirm that C15 substitution of blebbistatin does not substantially alter its inhibitory characteristics (Figure S1B,C).

To characterize the photostability of *para*-nitroblebbistatin, *para*-chloroblebbistatin, and blebbistatin, the effect of blue-light irradiation on their absorption spectra was compared (Figure 1E,F and Figure S1D). Upon irradiation, the absorption spectrum of blebbistatin changed markedly, which is consistent with previously published studies[3b,c,6] and indicates photoinduced changes in the molecular structure. The absorption spectra of the C15 chloro- and nitro-substituted derivatives of blebbistatin remained essentially unchanged upon blue-light irradiation.

We presumed that the improved photostability could be accompanied by a reduced phototoxic effect of the inhibitors. To test our hypothesis, we measured the blue-light-induced phototoxicity of the compounds on HeLa cells. The cells were treated with either *para*-nitroblebbistatin, *para*-chlorobleb-

 © 2014 Wiley-VCH Verlag GmbH & Co. KGaA, Weinheim

bistatin, or blebbistatin and then irradiated with blue light. The irradiation wavelength was 480 ± 10 nm, which is the most commonly used excitation range in fluorescence microscopy for GFP detection. The energy density was 3.3 μJ μm^{-2}, which is an average energy input in confocal microscopy applications (1–1400 μJ μm^{-2}).[3a] Following irradiation, the inhibitors were removed by washing and after 18 h of incubation the mortality rates were determined by trypan blue staining and subsequent counting of the cells. We observed no difference in the mortality and cell morphology in the nontreated control and *para*-nitroblebbistatin-treated cells, while blebbistatin treatment caused extensive cell death and led to a number of morphologically defective cells that were not stained by trypan blue (Figure 2A). *para*-Chloroblebbistatin treatment resulted in even more pronounced cell death than blebbistatin treatment (Figure S2). This result indicates that improved photostability is not necessarily accompanied by reduced phototoxicity.

To test the suitability of *para*-nitroblebbistatin for live-cell imaging, we performed a series of confocal microscopy experiments employing blue-light excitation. EGFP-α-tubulin mCherry-H2B-labeled HeLa Kyoto cells were imaged repeatedly over 12 h in a confocal microscope; three *z*-sections were applied every 10 min in the presence of 50 μM blebbistatin or *para*-nitroblebbistatin, which is a commonly applied concentration of blebbistatin. After blebbistatin treatment, the cells became defective as they did not enter into mitosis and most of them died or became morphologically seriously defective by the end of the experiment (Figure 2B, Movies S1–S3). Cells that were already in the mitotic phase before blebbistatin treatment, did not complete cytokinesis and formed multinuclear cells as a consequence of myosin II inhibition.[9] Additionally, fluorescent precipitates of blebbistatin hampered microscopic imaging. Cells treated with *para*-nitroblebbistatin did not show any sign of phototoxic damage and none of them died by the end of the experiment. The ratios of cells entering into the mitotic phase were the same in the *para*-nitroblebbistatin-treated cells as in the control experiment. Due to the myosin II inhibitory effect of *para*-nitroblebbistatin, all of the mitotic cells failed to perform cytokinesis and thus became multinuclear. Since *para*-nitroblebbistatin is not fluorescent, microscopic imaging was not perturbed by fluorescent aggregates.

In addition to experiments using HeLa cells, the phototoxicity of blebbistatin and *para*-nitroblebbistatin was also compared using *Danio rerio* (zebrafish) as a vertebrate model. Embryos 3 dpf (days post fertilization) in age were treated with the inhibitors at a concentration of 10 μM and irradiated with blue light (wavelength: 470 ± 20 nm, energy density: 0.4 μJ μm^{-2}). The mortality rate of the embryos was monitored for the following 36 h (Figure 2C). After 36 h the majority of the embryos that had received blebbistatin treatment were dead (86 ± 5%), whereas the mortality in the *para*-nitroblebbistatin-treated samples was significantly lower (18 ± 10%).

After elucidating that *para*-nitroblebbistatin is not phototoxic, we further evaluated its myosin II inhibition on different cellular systems. First, we compared the effect of *para*-nitroblebbistatin and blebbistatin on the cytokinesis of HeLa cells. The cells were treated with the inhibitors at a concentration of 20 μM and the change in cell number, viability, and the ratio of multinuclearity was monitored for 3 days (Figure 3A,B). Both inhibitors efficiently suppressed cytokinesis and therefore the initial cell number did not rise during the experiment. Consistently, the ratio of multinuclear cells continuously increased and by the third day, practically all cells were multinuclear. Blebbistatin treatment resulted in

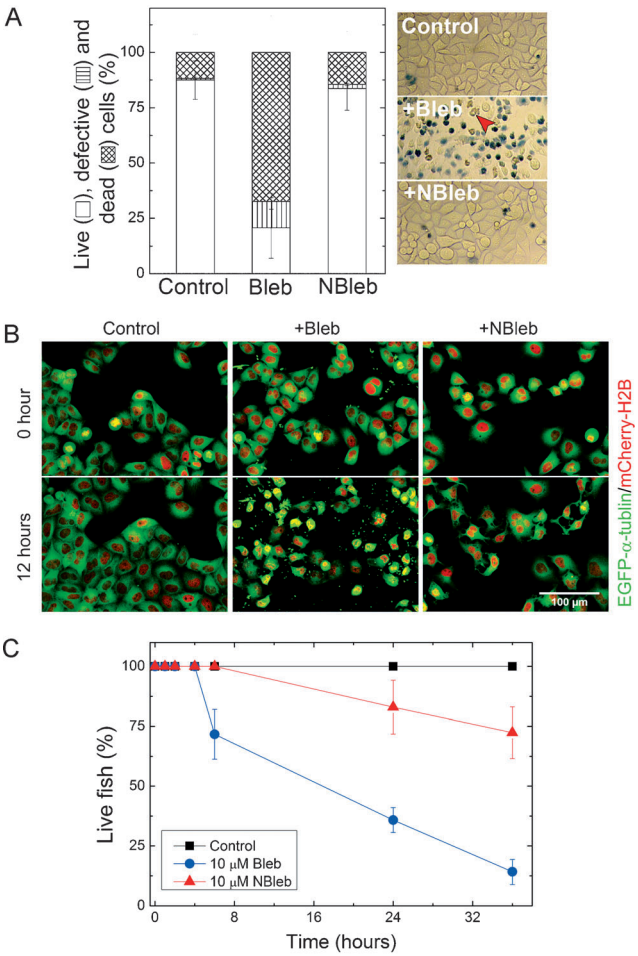

Figure 2. Phototoxicity of *para*-nitroblebbistatin and blebbistatin. A) HeLa cells were treated with 10 μM of NBleb or Bleb then irradiated at 480 ± 10 nm for 15 min along with untreated control cells. After the inhibitors had been removed by washing and the cells had been incubated for 18 h, the dead cells were stained with trypan blue and visualized by light microscopy (right panel). Live (unstained), dead (blue), and morphologically defective cells (red arrowhead) were counted and their ratios are presented in the column diagram (left panel, N = 350–400, mean values ± standard deviation). B) HeLa Kyoto cells were treated with DMSO (control), 50 μM NBleb, or Bleb and imaged repeatedly in a confocal microscope for 12 h. The excitation wavelengths were 488 and 543 nm for the GFP and mCherry, respectively. Most of the Bleb-treated cells became highly autofluorescent, which is an indication of cell death or serious defectiveness of cellular functions (Movies S1–S3). C) Zebrafish larvae (3 dpf in age) were treated with 10 μM NBleb or Bleb and irradiated at 470 ± 20 nm for 10 min along with untreated control larvae. Lifespans of the larvae were monitored for 36 h after treatment (N = 10, mean values ± standard deviation). All data represent at least three independent experiments.

© 2014 Wiley-VCH Verlag GmbH & Co. KGaA, Weinheim

a significant cell mortality, leading to 90% death ratio of HeLa cells in 3 days. Since the entire experiment was performed in the dark, this result reflects the cytotoxicity of blebbistatin in itself, without irradiation. In contrast, *para*-nitroblebbistatin did not affect the death rate of the cells. Additionally, the live blebbistatin-treated cells displayed severely defective cellular morphologies while *para*-nitroblebbistatin treatment did not damage the cells (Figure 3C). We further confirmed that *para*-nitroblebbistatin also induces multinuclearity of *Dictyostelium discoideum* (*Dd*) cells, similarly to blebbistatin (Figure S3). Neither of the inhibitors exerted cytotoxic effects on *Dd* cells. As blebbistatin was named after its characteristic effect of suppressing the blebbing of cells, we compared *para*-nitroblebbistatin and blebbistatin inhibition on this process as well by using the continuously blebbing M2 human melanoma cell line. Solutions of either compound at a concentration of 10 μM completely inhibited the blebbing within 10 min, and during this time no morphological difference was detected between cells treated with the inhibitors (Figure S4, Movies S4 and S5). These experiments demonstrate that *para*-nitroblebbistatin has the same in vivo specificity to nonmuscle myosin II as blebbistatin.

To explore the functional effects of *para*-nitroblebbistatin on vertebrates, we studied the development of the lateral line organ in zebrafish embryos, which involves nonmuscle myosin II function.[10] The lateral line is formed by pLLp (posterior lateral line primordia) cells migrating from the ear to the tip of the tail, meanwhile a series of mechanosensory receptors (neuromasts) are deposited regularly (Figure 4). Transgenic *cldnb:gfp* zebrafish embryos[11] with GFP-labeled pLLp and neuromasts were treated with increasing concentrations of *para*-nitroblebbistatin and blebbistatin starting at 1 dpf. After 24 h of incubation (at 2 dpf) the positions of the pLLp were studied. The treatment resulted in similar effects

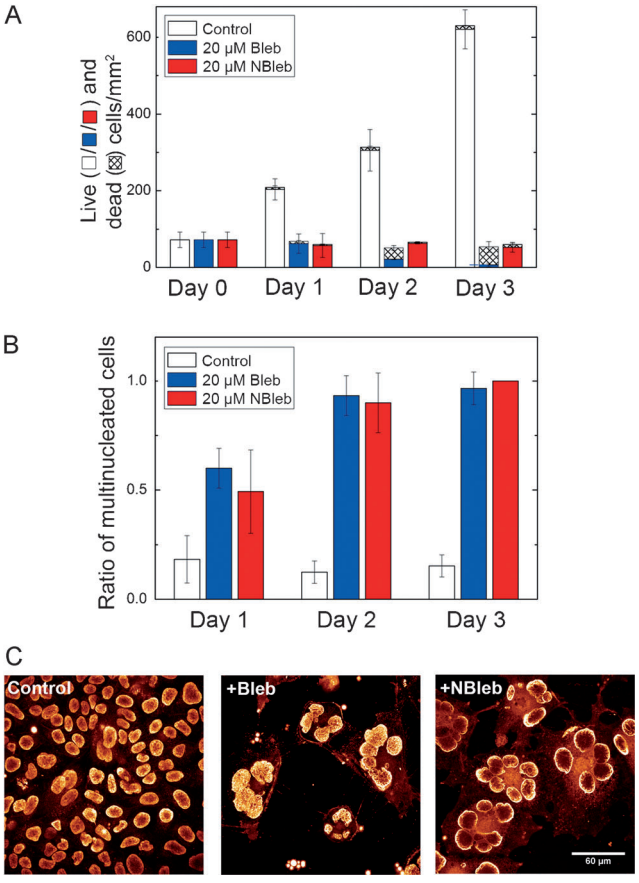

Figure 3. In vivo effects of *para*-nitroblebbistatin and blebbistatin on HeLa cells. A) HeLa cells were treated with 20 μM NBleb or Bleb and incubated for 3 days along with DMSO-treated control cells, while the changes in cell number and the rates of mortality were followed. B) HeLa cells were treated with 20 μM NBleb, Bleb, or DMSO and incubated for 3 days, while the ratio of their multinuclearity was followed. Data represent the mean values ± standard deviation of at least three independent experiments. C) Representative images of Hoechst-stained HeLa cells were taken on the third day of the experiment by confocal microscopy, excited at 405 nm wavelength.

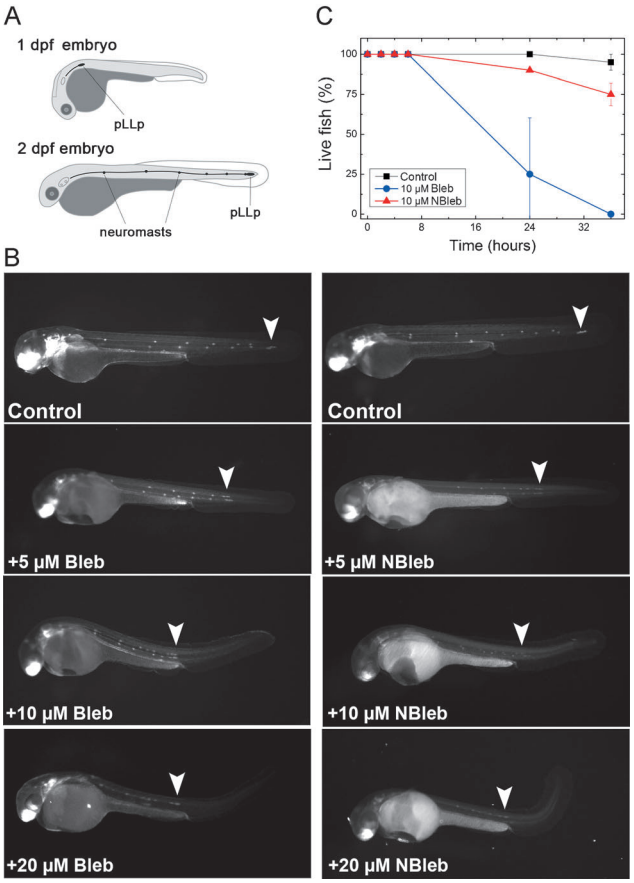

Figure 4. Comparison of the in vivo effects of *para*-nitroblebbistatin and blebbistatin on zebrafish embryos. A) The schematic representation depicts the migration of the lateral line primordium (pLLp) starting from the head region at 1 dpf heading to the tip of the tail while neuromasts are deposited regularly. The primordium cells are fluorescent due to the specific expression of claudin-GFP. B) 1 dpf embryos were treated with increasing concentrations of NBleb or Bleb and fluorescence stereomicroscope images (excitation wavelength 470 ± 20 nm) were recorded after 24 h of incubation. The migration fronts of pLLps are indicated by white arrowheads. C) Lifespans of 10 μM NBleb- or Bleb-treated and untreated embryos were monitored for 36 h ($N = 10$, mean values ± standard deviation from three independent experiments).

© 2014 Wiley-VCH Verlag GmbH & Co. KGaA, Weinheim

for both inhibitors, including the halt of the pLLp and a curved body shape (Figure 4B). However, animal mortality associated with blebbistatin administration was higher than that after *para*-nitroblebbistatin treatment. In 36 h the mortality rate of the *para*-nitroblebbistatin-treated embryos was similar to that of the nontreated control, whereas all fish died in the presence of 10 μM of blebbistatin. This reflects blebbistatin's high cytotoxicity in the dark which is a clearly different effect than its blue-light-induced phototoxicity (Figure 4C).

Here, we have demonstrated that the nitro substitution of blebbistatin at the C15 position decreases the fluorescence of the compound by a hundred times, increases the chemical stability upon blue-light irradiation, and greatly reduces its phototoxicity and cytotoxicity without affecting specific myosin II inhibitory properties. The analysis of the molecular structure of the myosin–ADP–vanadate–blebbistatin complex (PDB: 1YV3)[8] indicates that the nitro substituent at C15 does not significantly affect the interaction of the inhibitor with myosin, because the nitro substituent causes no steric hindrance for any of the side chains in the blebbistatin binding site of myosin (Figure 5).

The high cytotoxicity of blebbistatin, which irreversibly damages the in vivo systems even without blue-light irradiation, is a source of constant nuisance for experimental biologists. Furthermore, although the solubility of blebbistatin is around 20 μM (Figure S5), it is usually applied in vivo at concentrations of 50–100 μM. As the in vivo solubility of blebbistatin in the more hydrophobic cellular environment can be much higher than that measured in vitro, such high concentrations of the inhibitor induce nonspecific enzymatic interactions[7] and more pronounced cytotoxicity in in vivo experiments. Cytotoxicity and other nonspecific effects may easily lead to the misinterpretation of experimental results since myosin inhibition is interspersed with the side effects. Therefore, the non-cytotoxic, non-phototoxic, and nonfluorescent *para*-nitroblebbistatin is an ideal and complete replacement of blebbistatin for the study of the specific role of myosin II in physiological, developmental, and cell biological studies.

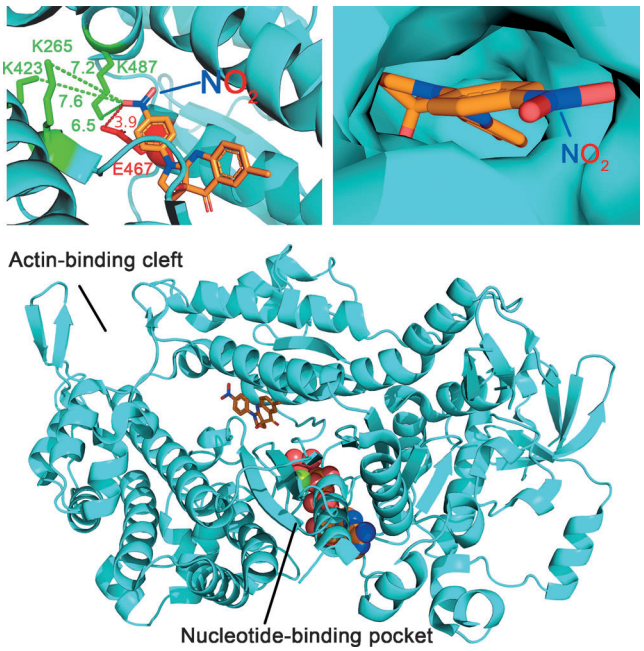

Figure 5. Structure of the myosin–ADP–vanadate–*para*-nitroblebbistatin complex. The model was created by the extension of Bleb with a nitro group at the C15 position in the crystal structure model of myosin–ADP–vanadate–blebbistatin (PDB: 1YV3). Myosin residues form a cavity halfway between the nucleotide-binding pocket and the actin-binding cleft, where the binding site of Bleb is situated (lower panel). Bleb and ADP–vanadate are shown by stick and space-filling representations, respectively. The possible attractive (green) and repulsive (red) interactions of the partially negatively charged nitro group of *para*-nitroblebbistatin are highlighted (upper left panel). The distance between the side chains of amino acids is indicated in Å. There is no steric hindrance between the additional nitro group and the myosin residues (upper right panel).

Received: March 20, 2014
Revised: May 2, 2014
Published online: June 20, 2014

Keywords: asymmetric synthesis · cytotoxicity · enzymes · inhibitors · proteins

[1] a) A. F. Straight, A. Cheung, J. Limouze, I. Chen, N. J. Westwood, J. R. Sellers, T. J. Mitchison, *Science* **2003**, *299*, 1743–1747; b) M. Kovacs, J. Toth, C. Hetenyi, A. Malnasi-Csizmadia, J. R. Sellers, *J. Biol. Chem.* **2004**, *279*, 35557–35563.

[2] a) S. G. Turney, P. C. Bridgman, *Nat. Neurosci.* **2005**, *8*, 717–719; b) A. J. Engler, S. Sen, H. L. Sweeney, D. E. Discher, *Cell* **2006**, *126*, 677–689; c) M. Krieg, Y. Arboleda-Estudillo, P. H. Puech, J. Käfer, F. Graner, D. J. Müller, C. P. Heisenberg, *Nat. Cell Biol.* **2008**, *10*, 429–436.

[3] a) T. Sakamoto, J. Limouze, C. A. Combs, A. F. Straight, J. R. Sellers, *Biochemistry* **2005**, *44*, 584–588; b) J. Kolega, *Biochem. Biophys. Res. Commun.* **2004**, *320*, 1020–1025; c) A. Mikulich, S. Kavaliauskiene, P. Juzenas, *Biochim. Biophys. Acta Gen. Subj.* **2012**, *1820*, 870–877.

[4] a) T. Kondo, K. Hamao, K. Kamijo, H. Kimura, M. Morita, M. Takahashi, H. Hosoya, *Biochem. J.* **2011**, *435*, 569–576; b) C. S. Rex, C. F. Gavin, M. D. Rubio, E. A. Kramar, L. Y. Chen, Y. Jia, R. L. Huganir, N. Muzyczka, C. M. Gall, C. A. Miller, G. Lynch, G. Rumbaugh, *Neuron* **2010**, *67*, 603–617.

[5] K. Wong, A. Van Keymeulen, H. R. Bourne, *J. Cell Biol.* **2007**, *179*, 1141–1148.

[6] C. Lucas-Lopez, S. Patterson, T. Blum, A. F. Straight, J. Toth, A. M. Z. Slawin, T. J. Mitchison, J. R. Sellers, N. J. Westwood, *Eur. J. Org. Chem.* **2005**, 1736–1740.

[7] M. Kepiro, B. H. Varkuti, A. Bodor, G. Hegyi, L. Drahos, M. Kovacs, A. Malnasi-Csizmadia, *Proc. Natl. Acad. Sci. USA* **2012**, *109*, 9402–9407.

[8] J. S. Allingham, R. Smith, I. Rayment, *Nat. Struct. Mol. Biol.* **2005**, *12*, 378–379.

[9] S. Shu, X. Liu, E. D. Korn, *Proc. Natl. Acad. Sci. USA* **2005**, *102*, 1472–1477.

[10] a) S. Ernst, K. Liu, S. Agarwala, N. Moratscheck, M. E. Avci, D. Dalle Nogare, A. B. Chitnis, O. Ronneberger, V. Lecaudey, *Development* **2012**, *139*, 4571–4581; b) M. J. Harding, A. V. Nechiporuk, *Development* **2012**, *139*, 3130–3135.

[11] P. Haas, D. Gilmour, *Dev. Cell* **2006**, *10*, 673–680.

 © 2014 Wiley-VCH Verlag GmbH & Co. KGaA, Weinheim